First-principles study of the magnetic structures of ordered and disordered Mn-Ir alloys

A. Sakuma
Advanced Electronics Research Laboratory, Hitachi Metals, Ltd., 5200 Mikajiri, Kumagaya, Saitama, 360-0843 Japan

K. Fukamichi, K. Sasao, and R. Y. Umetsu
Department of Materials Science, Graduate School of Engineering, Tohoku University, Aoba-yama 02, Sendai, 980-8579 Japan
(Received 26 June 2002; published 23 January 2003)

Electronic and magnetic structures of γ-phase disordered $Mn_{100-x}Ir_x$ alloys including $L1_2$-type ordered Mn_3Ir alloy have been investigated by the first-principles approach using the tight-binding (TB) linear muffin tin orbital (LMTO) method. For the $L1_2$-type ordered Mn_3Ir alloy, a triangular ($T1$) magnetic structure is considered to be stable, reflecting in a dip structure around the Fermi level in the density of states. For the γ-phase disordered Mn_3Ir alloy, on the other hand, the most stable structure is suggested to be the $3Q$ structure among the multiple-Q spin density wave (MSDW) structures. The Néel temperature is estimated to be about 735 K from the effective exchange constant J_0, in good agreement with the experimental value of about 730 K. With decreasing Ir concentration in the γ-phase disordered $Mn_{100-x}Ir_x$ alloys, the transition from the $3Q$ to the $2Q$ structure takes place in the vicinity of $x=13$ under the constant lattice parameters with the axial ratio of $c/a=1$. This critical concentration x is close to the observed concentration at which the axial ratio changes from $c/a=1$ to $c/a>1$. However, it should be stressed that these two critical concentrations do not necessarily coincide with each other, that is, the critical concentration of the magnetic structure transition is lower than that of the lattice distortion. This theoretical expectation has been verified by the experimental structural and magnetic data.

DOI: 10.1103/PhysRevB.67.024420 PACS number(s): 75.25.+z, 75.50.Ee, 71.20.Be

I. INTRODUCTION

Magnetic structures of γ-phase Mn-based alloys have still been far from understanding and studied for a few decades in connection with the lattice distortion which varies with the concentration of additional elements such as Cu,[1] Ni,[2,3] Pd,[4] Ir,[5] Rh,[6] and Fe.[7] Experimentally, for example, it has been reported that the axial ratio c/a in γ-phase $Mn_{100-x}M_x$ ($M \equiv$Ni and Rh) alloys changes in the sequence of $c/a<1$, $a>b>c$, $c/a>1$ and $c/a=1$ with increasing concentration x.[3,6] The concentration dependence of the Néel temperature T_N is different, depending on the additional element. That is, T_N increases in Mn-Ir (Refs. 5 and 8), Mn-Rh (Refs. 6, 9, and 10), and Mn-Ru (Refs. 11 and 12) systems, while T_N decreases with increasing x in Mn-Cu (Ref. 1), Mn-Ni (Refs. 2 and 3), Mn-Pd (Ref. 4), Mn-Fe (Ref. 7), Mn-Au (Ref. 13), and Mn-Pt (Ref. 14) systems. These concentration dependences have been explained by the number of $3d$ electrons in the Mn site, which is calculated by the linear muffin-tin orbital atomic sphere approximation.[10] For the magnetic structures, however, no systematic detailed investigations have been made because of some experimental and theoretical difficulties.

Practically, on the other hand, several kinds of antiferromagnetic Mn-based alloy systems have been investigated intensively as an exchange biasing film in the giant magnetoresistance (GMR) and tunnel magnetoresistance (TMR) devices. Especially, γ-phase disordered Mn-Ir alloys exhibit the Néel temperature enough high for these devices without postannealing.[15–18] Therefore, γ-phase disordered Mn-Ir alloys are considered as one of the most promising candidates for the exchange coupling film of spin valves[15,16] and magnetic tunnel junctions.[17–19] It is important to note that the exchange biasing and the blocking temperature characteristics are intimately related to the magnetic structures.[20–22] Accordingly, fundamental studies of antiferromagnetic Mn-based alloys are strongly desired to develop excellent properties for GMR and TMR devices.

The lattice constants and the Néel temperatures of γ-phase disordered $Mn_{100-x}Ir_x$ alloys were first investigated by Yamaoka.[5] He demonstrated that the Néel temperature of the disordered alloy around $x=25$ is very high, of about 730 K among several kinds of Mn-based alloy systems. A recent study by Tomeno *et al.*[23] showed that $L1_2$-type ordered Mn_3Ir alloy also has a high Néel temperature of about 950 K. On the other hand, no systematic theoretical investigations have been performed yet for Mn-based alloys, except for $L1_2$-type ordered Mn_3Pt and Mn_3Rh alloys.[24] The magnetic structure of the latter two ordered alloys was suggested to be the so-called triangular ($T1$) structure from both experimental[14,25] and theoretical[24] works.

In the previous studies based on the first-principles calculations, we have suggested within the frame of the coherent potential approximation (CPA) that disordered FeMn and MnPt alloys have a $3Q$ spin density wave structure,[26] though the $3Q$ structure is most unstable in the multiple-Q spin density wave (MQSDW) structures in pure γ-Mn metal.[27] From theoretical point of view, therefore, the magnetic structure of Mn-based alloys such as γ-phase disordered Mn-Ir alloys would attract much attention in the sense how the composition ratio influences the magnetic structure.

In the present work, the electronic and the magnetic structures of disordered $Mn_{100-x}Ir_x$ ($0 \leqslant x \leqslant 30$) and ordered Mn_3Ir alloys are calculated by the tight-binding (TB) linear muffin tin orbital (LMTO) method based on the local spin density (LSD) functional approximation. A brief explanation

of the theoretical methodology will be presented in the following section and its more detailed description was already given in Ref. 26. In order to shed light on the intrinsic effects of the addition of Ir atoms, first we fix the lattice constants at the observed value for $x=25$ with the axial ratio of $c/a=1$, and then the effects of the lattice distortion will be discussed. Next, the effective exchange constant[26,28] acting on each Mn moment is also calculated to examine the magnetic stability and to estimate the Néel temperature. Finally, structural and magnetic properties have experimentally been investigated in order to verify the theoretical expectation for the discordance between the compositions of the magnetic structure change and the crystallographic structure change.

II. CALCULATION METHOD

Since detailed procedures for calculations have been described elsewhere,[26] we give a brief explanation in this section. In the TB-LMTO method,[29] the Green function (GF) is given by the following equation:

$$\overline{G}(\omega)=\Delta^{-1/2}g^{\gamma}(\omega)\Delta^{-1/2} \tag{1}$$

where $g^{\gamma}(\omega)=[p^{\gamma}(\omega)-\overline{S^{\gamma}}]^{-1}$ is the so-called auxiliary GF composed of the potential function $p^{\gamma}(\omega)$ and the screened structure constants $\overline{S^{\gamma}}$ given by $p^{\gamma}(\omega)=\{(\omega-C)/\Delta\}\delta_{L',L}\delta_{\sigma',\sigma}$ and $\overline{S^{\gamma}}=\overline{S}(1-\gamma\overline{S})^{-1}$, respectively. Here we define $L=(i,l,m)$ (i denotes the site, l and m are orbital indices) and σ as the spin state. The quantities C, Δ, and γ are the potential parameters in each atomic sphere determined by using the LSD. The local spin quantization axis pointing to (θ_i,φ_i), namely, the direction of magnetic moment on the ith site, is introduced in $\overline{S}$ through $\overline{S}_{L'\sigma',L\sigma}=(U(\theta_{i'},\varphi_{i'})S_{L',L}U^{+}(\theta_i,\varphi_i))_{\sigma',\sigma}$ with the spin rotation matrix U. The site-diagonal part (i,i component) of the GF in Eq. (1) is diagonal with respect to the spin space, because the GF in Eq. (1) is defined in the local frame of the spin axis.

Applying the CPA to the disordered alloys, the most localized (β) representation[30,31] is used for the potential function and the structure constants through the transformation as $p^{\beta}=p^{\gamma}[1-(\beta-\gamma)p^{\gamma}]^{-1}$, $\overline{S^{\beta}}=\overline{S^{\gamma}}[1-(\beta-\gamma)\overline{S^{\gamma}}]^{-1}=\overline{S}(1-\beta\overline{S})^{-1}$ with $\beta_{l=0}=0.3485$, $\beta_{l=1}=0.0530$, $\beta_{l=2}=0.0107$. From these quantities, the CPA condition for the system constituted of plural sublattices is given as

$$\langle T_i\rangle=\sum_a c_{ia}[p^{\beta}_{ia}(\omega)-\tilde{p}_i(\omega)]\times\{1+[p^{\beta}_{ia}(\omega)-\tilde{p}_i(\omega)]\Phi_i(\omega)\}^{-1}=0, \tag{2}$$

with $\Phi_i(\omega)=(1/N)\Sigma_k[(\tilde{p}(\omega)-\overline{S^{\beta}_k})^{-1}]_{ii}$, where $\tilde{p}_i(\omega)$ is the coherent potential function, c_{ia} denotes the density (probability) of a atom occupying the sublattice i. After the self-consistent calculation for the a atom at the ith sublattice, the auxiliary GF in the β representation is given by

$$g^{\beta}_{ia}(\omega)=\Phi_i(\omega)\{1+[p^{\beta}_{ia}(\omega)-\tilde{p}_i(\omega)]\Phi_i(\omega)\}^{-1}. \tag{3}$$

We can obtain the auxiliary GF $g^{\gamma}(\omega)$ in the local frame of the spin axis by transforming from the β representation to the γ representation by using the following identity equation:

$$g^{\gamma}=(p^{\gamma})^{-1}-(p^{\gamma})^{-1}p^{\beta}(p^{\gamma})^{-1}+(p^{\gamma})^{-1}p^{\beta}g^{\beta}p^{\beta}(p^{\gamma})^{-1}. \tag{4}$$

Being obtained the auxiliary GF $g^{\gamma}(\omega)$, the effective exchange constant regarded as the amplitude of the exchange field acting on an atom denoted by 0 by surrounding moments, $J_0=(\Sigma_{i\neq 0}J_{i0}\mathbf{e}_i)\cdot\mathbf{e}_0$, is expressed by

$$J_0=-\frac{1}{4\pi}\mathrm{Im}\int^{E_F}d\omega\,\mathrm{Tr}_{lm}\{\Omega_0(\omega)[g^{\gamma\uparrow\uparrow}_{00}(\omega)-g^{\gamma\downarrow\downarrow}_{00}(\omega)]+\Omega_0(\omega)g^{\gamma\uparrow\uparrow}_{00}(\omega)\Omega_0(\omega)g^{\gamma\downarrow\downarrow}_{00}(\omega)\} \tag{5}$$

with $\Omega_i(\omega)\equiv[p^{\uparrow}_i(\omega)-p^{\downarrow}_i(\omega)]$. It should be noted that this equation is also valid for the noncollinear magnetic structures in both ordered and disordered alloys.[26] Furthermore, the Néel temperature T_N is given by the following expression from a generalized molecular field theory by Liechtenstein *et al.*:[28]

$$T_N=\frac{2J_0}{3k_B}. \tag{6}$$

III. EXPERIMENT

Several kinds of $Mn_{100-x}Ir_x$ alloys were prepared by arc melting in Ar gas atmosphere. For homogenization, the specimens were sealed with Ar gas in quartz tubes and annealed at 1273 K for 3 days, subsequently quenched into ice water.

The crystal structures and the lattice constants were examined by x-ray powder diffraction using Cu- $K\alpha$ radiation. The alloy compositions were confirmed by an inductively coupled plasma (ICP) analysis and also decided from the density with the lattice constants. The temperature dependence of magnetic susceptibility χ was measured with a superconducting quantum interference device (SQUID) magnetometer from 10 to 400 K and with a vibrating sample magnetometer (VSM) from 300 to 1000 K in a magnetic field of 10 kOe.

IV. RESULTS AND DISCUSSION

A. Electronic and magnetic structures of the $L1_2$-type ordered and the γ-phase disordered Mn_3Ir alloys

There are two kinds of crystal structures for Mn_3Ir alloys: $L1_2$-type (γ-phase) ordered (O) and γ-phase disordered (DO) alloys. Let us first show the local density of states (DOS) of the $L1_2$-type ordered (O) Mn_3Ir alloy in Fig. 1, together with the magnetic structure called the triangular ($T1$) structure proposed by Kouvel and Kasper[25] and Krén *et al.*[14] for ordered Mn_3Rh and Mn_3Pt alloys. The Mn moments are parallel to the (111) plane and aligned in the $\langle 112\rangle$ direction. The magnetic structure of the $L1_2$-type ordered Mn_3Ir has been identified as the same.[23] In the present calculations, the lattice constant is settled at 3.785 Å from the

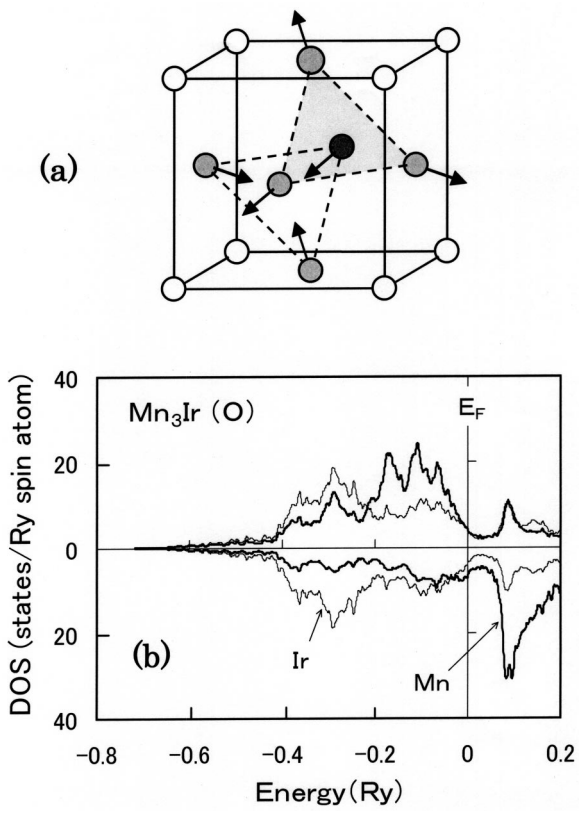

FIG. 1. Triangular ($T1$) magnetic structure (a) and the local density of states (b) of the $L1_2$-type ordered (O) Mn_3Ir alloy. The crossed and open circles stand for Mn and Ir atoms, respectively. The upper and lower curves refer to the majority and minority spin states, respectively, for the Mn and Ir sites.

experimental data.[5] The moment of the Mn atom is $2.62\mu_B$ and that of Ir is zero. For comparison, shown in Fig. 2 is the local DOS in a disordered local moment (DLM) state as the paramagnetic (PM) state, in which the Mn moments pointing upward [Mn(↑)] and downward [Mn(↓)] are randomly distributed in each Mn sublattice. The Mn moment is reduced to $2.20\mu_B$ whereas the behavior of the local DOS below -0.1

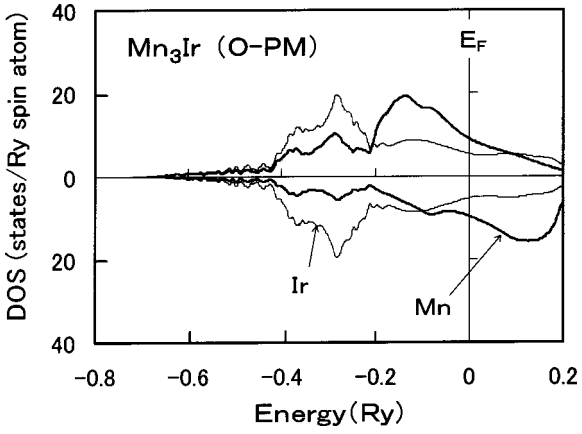

FIG. 2. Local density of states of the $L1_2$-type ordered (O) Mn_3Ir alloy in the disordered local moment (DLM) state in the paramagnetic (PM) state.

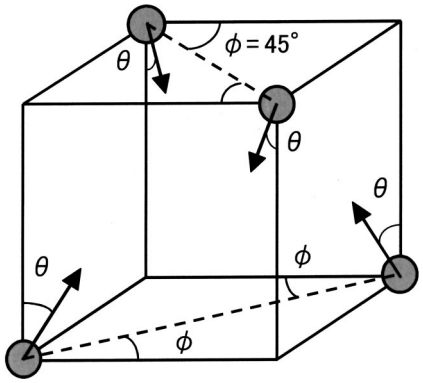

FIG. 3. Multiple-Q spin density wave (MQSDW) structures in the magnetic primitive cell of an fcc lattice.

Ry is retained in both the $T1$ and the PM states, and the dip around the Fermi energy E_F found in the $T1$ state is swept out in the PM state. This situation is similar to that of $L1_0$-type equiatomic MnPt alloy[26] in which the pseudogap realized in the antiferromagnetic state completely vanishes in the PM state, which means that the gap is closely connected with the antiferromagnetic long-range order. The energy in this PM state is higher than that of the $T1$ state as much as 6 mRy/atom.

To bear out the magnetic stability in the $T1$ state, the effective exchange constant J_0 in Eq. (5) is calculated for the $L1_2$-type ordered (O) Mn_3Ir alloy. The value of J_0 is about 160 meV, and hence Eq. (6) gives the Néel temperature of 1250 K, higher by about 30% than the experimental data.[23] Such a higher value would be adequate within the molecular field approximation for three-dimensional systems. Similar discrepancies have been observed in Mn alloys and compounds.[27,32]

Figure 3 shows the magnetic structure of the γ-phase disordered alloys, indicating a magnetic primitive cell constituted of four atoms in the fcc structure. Note that the angles θ and ϕ are defined individually for each site. When ϕ is settled at 45°, $\theta=0°$, $\theta=\cos^{-1}(1/\sqrt{3})=54.7°$, and $\theta=90°$ correspond to the so-called $1Q$, $3Q$, and $2Q$ spin density wave (SDW) structures, respectively, which are generally called the multiple-Q SDW (MQSDW) structures.[24,33–36] The magnetic structure in the disordered alloys considered here is restricted within MQSDW structures; $1Q$, $2Q$, and $3Q$ in the fcc lattice. Given in Fig. 4 are the DOS's of each magnetic structure in (a), (b), and (c), and the inset in each figure refers to the corresponding magnetic structure for the disordered (DO) Mn_3Ir alloy. The lattice parameter is settled at $a=3.785$ Å. Contrary to the results of the $L1_0$-type MnPt alloy considered in our previous work,[26] the local DOS of Mn and Ir sites well maintains the characteristic features of DOS of the $T1$ structure in the ordered alloy. Especially, it should be marked that DOS of the $3Q$ structure is most close to the $T1$ structure and exhibits a large dip around E_F, which is comparable to the ordered alloy. Therefore, it is considered that the $3Q$ structure in the disordered alloy has a lower energy, compared with the DLM state as the PM state for the $L1_2$-type ordered alloy. The relative difference between the total energy of the magnetic structures is presented in Table

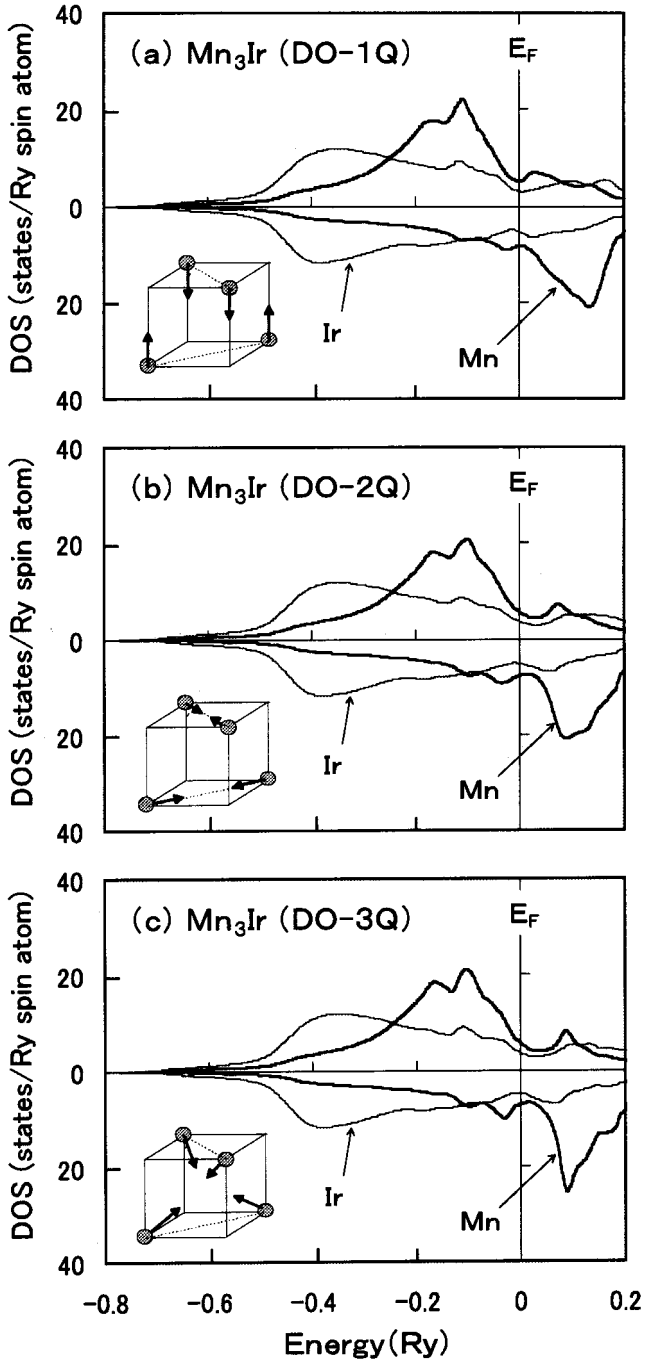

FIG. 4. Density of states of the γ-phase disordered (DO) Mn_3Ir alloy for each magnetic structure. Note that the slight difference between the majority and minority spin states for the Ir sites gives a small magnetic moment (see Table I). The inset in each figure refers to the corresponding magnetic structure. (a) $1Q$ structure, (b) $2Q$ structure, (c) $3Q$ structure.

I. Coming up to our expectation, the $3Q$ state in the γ-phase disordered (DO) alloy is more stable by about 0.1 mRy/atom than that in the PM state in the $L1_2$-type ordered (O) alloy.

In Table I, we also show the effective exchange constant J_0 of each MQSDW structure for the disordered (DO) Mn_3Ir alloy. The order of magnitude of J_0 in these magnetic structures is consistent with the relative difference in the energy.

TABLE I. The magnetic structure, calculated total energy (ΔE in mRy/atom), magnetic moment (M in μ_B), effective exchange constant (J_0 in meV), and Néel temperature (T_N^{calc} in K) estimated from $2J_0/3k_B$ for the $L1_2$-type ordered (O) and the γ-phase disordered (DO) Mn_3Ir alloys. The experimental values of the Néel temperature T_N^{expt} are also given for comparison.

Phase	Magnetic structure	ΔE	M_{Mn}	M_{Ir}	J_0	T_N^{calc}	T_N^{expt}
$L1_2$ type	$T1$	0	2.62	0.00	162	1253	960[23]
(O)	PM	5.7	2.20	0.00			
γ phase	$1Q$	6.9	2.46	0.09	41	317	730[5]
(DO)	$2Q$	6.0	2.47	0.11	85	66	
	$3Q$	5.6	2.51	0.12	95	0	
	PM	14.8	2.27	0.00		735	

Therefore, the present results imply that the $3Q$ structure is most stable in the γ-phase disordered alloy. Indeed, as shown in Table I, the $3Q$ state in the disordered (DO) alloys is more stable than the PM state in the ordered (O) alloy. This is in contrast to the $L1_0$-type MnPt alloy where the MQSDW structures in the disordered alloy have a higher energy than in the PM state of the ordered alloy.[26] In the table, the energy of the PM state in the disordered (DO) state is also shown by using the CPA for the random alloy of the composition $Mn(\uparrow)_{0.375}Mn(\downarrow)_{0.375}Ir(\uparrow)_{0.125}Ir(\downarrow)_{0.125}$. The energy in the PM state is higher by about 8 mRy/atom than that in the MQSDW states, which means that the MQSDW states in the disordered (DO) alloy are stable in analogy with the $T1$ state in the ordered (O) alloy. The Néel temperature estimated from J_0 is about 735 K, in accord with the experimental value of about 730 K,[5] though the present result for the stable $3Q$ magnetic structure is different from the $1Q$ structure suggested by Yamaoka, Mekata, and Takaki.[37] For the discrepancy between the spin structures, one may notice that powder neutron diffractions are unable to distinguish between the $1Q$ and the $3Q$ structure. In addition, the slight difference between the DOS in the majority and minority spin states results in a small magnetic moment for Ir atom as given in the table.

B. Concentration dependence of the magnetic structure of the γ-phase disordered $Mn_{100-x}Ir_x$ alloy system

In the previous work,[27] one of the present authors pointed out that the $3Q$ structure is most unstable and the $2Q$ structure seems to be preferable among the MQSDW structures in pure γ-Mn metal with $c/a=1$, whereas the γ-phase disordered Mn_3Ir alloy turns out to prefer the $3Q$ structure as predicted in the preceding subsection. Furthermore, it has been shown that neither the lattice expansion nor the lattice distortion in pure γ-Mn metal can lead to the $3Q$ structure,[27] which convinces ourselves that the addition of Ir atoms is responsible for the $3Q$ structure. The questions arise as to how and where the composition the $2Q$ structure in the pure γ-Mn metal changes to the $3Q$ structure in the γ-phase disordered alloy.

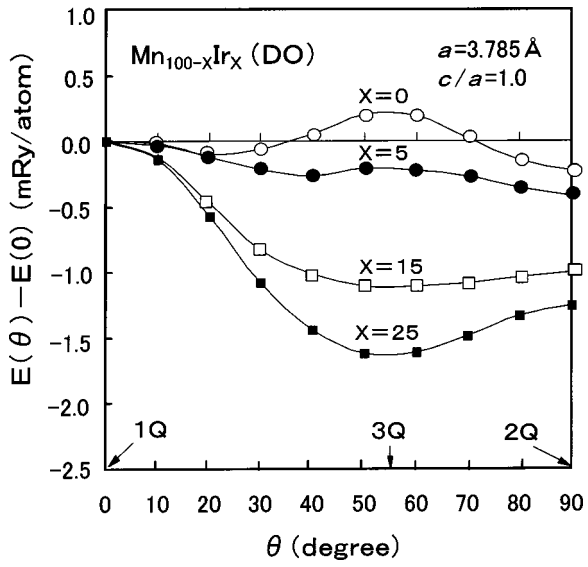

FIG. 5. The θ dependence of the electronic total energy for $x=0$, 5, 15, and 25 in the γ-phase disordered (DO) $Mn_{100-x}Ir_x$ alloys. The lattice constant is fixed at $a=3.785$ Å.

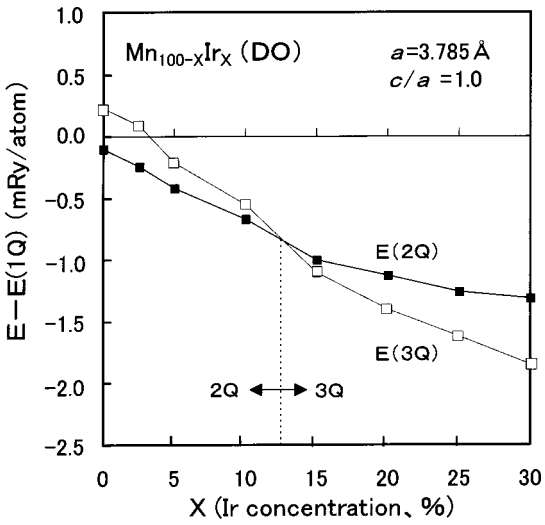

FIG. 6. Concentration dependence of the electronic total energy of the γ-phase disordered (DO) $Mn_{100-x}Ir_x$ alloys for the $2Q$ and the $3Q$ structures. The total energy is given relative to that of the $1Q$ structure.

To investigate systematically the variation of energy with the change of the magnetic structure, the electronic total energy for several compositions of x in the γ-phase disordered $Mn_{100-x}Ir_x$ alloys are plotted in Fig. 5 as a function of angle θ defined in Fig. 3. Note that $\theta=0°$, 54.7°, and 90° correspond to the $1Q$, the $3Q$ and the $2Q$ structures, respectively, as explained in connection with Fig. 3. The lattice constant is fixed at $a=3.785$ Å and the axial ratio c/a is also fixed at unity. The curve of $x=0$ indicates that the $2Q$ structure ($\theta=90°$) is most stable and the $3Q$ structure ($\theta=54.7°$) has a maximum energy in analogy with the previous results for pure γ-Mn metal.[27] Noteworthy is that only 5% addition of Ir atoms makes the energy of the $3Q$ structure lower than that of the $1Q$ structure. The energies of both the $2Q$ and the $3Q$ structures are lowered relative to that of the $1Q$ structure with increasing x. Figure 6 shows the concentration dependence of the total energy of the $2Q$ and the $3Q$ structures relative to that of the $1Q$ structure. The total energies both of the $2Q$ and the $3Q$ structures exhibit a monotonic decrease with x. The slope is steeper in the $3Q$ structure than that in the $2Q$ structure, intersecting at the concentration x between 10 and 15. Thus, the $2Q$ structure is stable until x of about 13 and the $3Q$ structure is found to be realized in $x>13$. Returning to Fig. 5, we can confirm that there is no intermediate state between the $2Q$ and the $3Q$ structure as the ground state, that is, the curves exhibit no minimum in the range $54.7°<\theta<90°$, and hence the transition is of the first order.

Emphasis to be placed on the results in Fig. 6 is that the Ir concentration where the magnetic transition from the $2Q$ to the $3Q$ structure takes place is quite close to the concentration at which the axial ratio changes from $c/a>1$ to $c/a=1$, which was observed by Yamaoka.[5] It was predicted that even in the pure γ-Mn metal, the lattice distortion of $c/a>1$ further lowers the total energy of the $2Q$ structure.[27] Actually, we have confirmed from the calculations that the total energy of the $2Q$ structure in the γ-phase disordered $Mn_{85}Ir_{15}$ alloy becomes lower than that of the $3Q$ structure when the lattice is distorted to $c/a=1.05$, whereas the $3Q$ structure in the γ-phase disordered $Mn_{80}Ir_{20}$ alloy is still stable under the same condition of $c/a=1.05$. Thus, it can be inferred that the critical concentration defined by x_m for the magnetic transition is put forward to a higher concentration by a few percent if the constraint for the lattice distortion is free. It should be marked, however, that the concentration x_m does not necessarily coincide with the concentration defined by x_t for the lattice distortion. This can be understood by noting a situation that the γ-phase disordered $Mn_{80}Ir_{20}$ alloy with the $3Q$ structure is found to prefer $c/a>1$ energetically rather than $c/a=1$, while for the γ-phase disordered $Mn_{75}Ir_{25}(\equiv Mn_3Ir)$ alloy the lattice keeps $c/a=1$ with the $3Q$ structure. From these relations, one can expect that x_t is higher than x_m. This is because the lattice distortion of $c/a>1$ lowers not only the total energy of the $2Q$ structure but also that of the $3Q$ structure. When the total energy of the $3Q$ structure is low enough in $c/a=1$, any degree of the lattice distortion cannot always cause a reversal from the $3Q$ to the $2Q$ magnetic structure. It should be noted that Fishman *et al.* have confirmed the difference between the magnetic and structural transition temperatures for Mn-Ni alloy system.[38] They further predicted by a phenomenological model that there should exist, between x_t and x_m for $c/a>1$, another magnetic structure denoted by T-SDW phase where the moments tilt from the $3Q$ structure towards the $2Q$ structure. We stress that this is possibly true because we observe in our calculation that the angle corresponding to the $3Q$ structure (54.7°) slightly shifts toward 90° ($2Q$ structure) when the lattice is distorted to $c/a>1$. However, we do not make further insight into the magnetic structure including the lattice distortion in the quantitative stage, because of limitation of the accuracy of the present methods; the TB-LMTO method together with the local spin density (LSD) functional approximation.

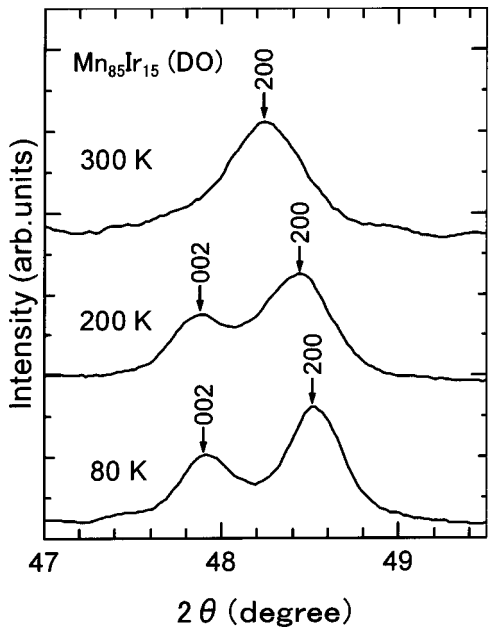

FIG. 7. X-ray diffraction patterns for the γ-phase disordered (DO) $Mn_{85}Ir_{15}$ alloy at 80, 200, and 300 K. Note that the fct structure is observed at 80 and 200 K, whereas the fcc structure is observed at 300 K.

We have experimentally reinvestigated the Mn-Ir alloy system in order to establish the structural and magnetic phase diagram and to verify the discussion in connection with Fig. 6. Figure 7 shows the representative x-ray diffraction patterns at 80, 200, and 300 K for the disordered $Mn_{85}Ir_{15}$ alloy. The face-centered tetragonal (fct) structure with $c/a>1$ is observed at 80 and 200 K, whereas the face-centered cubic (fcc) structure is observed at 300 K. Temperature dependence of the magnetic susceptibility measured in a field of 10 kOe for the same specimen of the disordered $Mn_{85}Ir_{15}$ alloy is given in Fig. 8. No anomaly is observed in the magnetic susceptibility at the structural phase transition temperature from the fct to the fcc, $T_{\mathrm{fct/fcc}}$, which was confirmed by x-ray diffraction measurement. Fishman and Liu have calculated the magnetic susceptibility of γ-Mn alloys and pointed out that the average susceptibilities are different depending on the magnetic structures.[36] Thus the transition from the high-temperature $3Q$ phase to the low-temperature $2Q$ phase, the magnetic susceptibility is clearly reduced by a few percent below the transition temperature $T_{2Q/3Q}$. Therefore, the apparent decrease in the magnetic susceptibility at low temperatures in the present result is identified as the magnetic structure change as discussed by Fishman and Liu.[36]

Figure 9 shows our new Mn-Ir phase diagram, together with the results reported by Yamaoka.[5] The Néel temperature at $x=0$ given by the open triangle is an extrapolated value for Mn-Fe-Cu alloy system.[7] The point to observe is that the lattice distortion from $c/a=1$ to $c/a>1$ for the present result given by the solid line takes places at higher concentration by a few percent, compared with that data given by the dash-dotted lines from Yamaoka,[5] supporting more strongly the theoretical discussion given above. In addition, the data of the Néel temperature obtained by Yamaoka practically

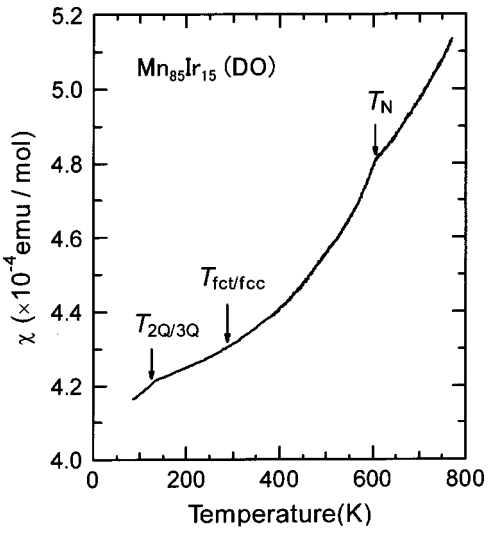

FIG. 8. Temperature dependence of the magnetic susceptibility for the γ-phase disordered (DO) $Mn_{85}Ir_{15}$ alloy. The magnetic transition temperature from $2Q$ to $3Q$, $T_{2Q/3Q}$, the structural phase transition temperature from fct to fcc $T_{\mathrm{fct/tcc}}$, and the Néel temperature T_{N} are given by the arrows.

overlap with the present data by shifting about a few percent. In chemical analyses, strong insolubility of Ir seems to be the reason for the discrepancies given in Fig. 9. Furthermore, a new distorted phase with $a>b>c$ has been confirmed by x-ray diffraction as shown by the dotted line in the same figure. What has to be noticed is that the phase diagram of Mn-Ir alloy system is similar to that of Mn-Rh,[6] though the tetragonal phase with $c/a<1$ is not confirmed below about 7% Ir because of an easy appearance of a β phase.

V. CONCLUSION

The electronic and the magnetic structures of the $L1_2$-type ordered Mn_3Ir and the γ-phase disordered $Mn_{100-x}Ir_x$ alloys have been investigated by the tight-

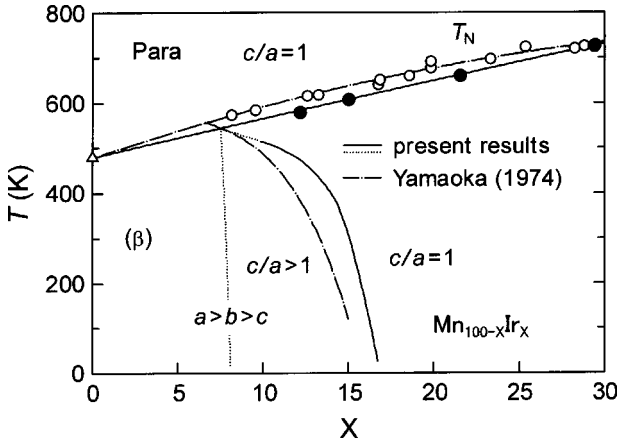

FIG. 9. The phase diagram of the Néel temperature T_{N} and the crystal structure for Mn-Ir system, together with that reported by Yamaoka (Ref. 5). The present data are given by the solid and the dotted lines together with the closed circles. The dash-dotted lines and the open circles are from Yamaoka (Ref. 5).

binding (TB) linear muffin tin orbital (LMTO) method. The magnetic stability in both systems is also examined with the effective exchange constants acting on the Mn moments. The long-range order with the $T1$ structure in the ordered Mn_3Ir alloy is reflected in a dip structure around the Fermi level of the density of states (DOS). This characteristic feature can be retained in the multiple-Q spin density wave (MQSDW) structures in the γ-phase disordered (DO) Mn_3Ir alloy, implying that an antiferromagnetic long-range order also remains in the disordered alloy. The most stable structure in the γ-phase disordered $Mn_{75}Ir_{25}$ ($\equiv Mn_3Ir$) alloy is suggested to be the $3Q$ structure. The Néel temperature converted from the effective exchange constant J_0 is about 735 K, in good agreement with the experimental value of about 730 K. On the other hand, the Néel temperature of the $L1_2$-type ordered Mn_3Ir alloy is considerably higher by about 30% than the experimental value of about 950 K.

With decreasing x in the γ-phase disordered $Mn_{100-x}Ir_x$ alloy system, the transition from the $3Q$ to the $2Q$ structure takes place in the vicinity of $x=13$ under the constant lattice parameters with the axial ratio of $c/a=1$. This critical concentration x is close to the observed concentration at which the axial ratio changes from $c/a=1$ to $c/a>1$ with decreasing x. However, it should be emphasized that these two critical compositions do not always coincide with each other. In other words, the concentration of the magnetic structure transition is lower than that of the lattice distortion; because there is a concentration region where the $3Q$ structure is still stable even though $c/a>1$. This situation has been verified experimentally. The concentration dependence of the Néel temperature obtained by Yamaoka practically overlap with the present data by shifting about a few percent.

ACKNOWLEDGMENTS

The present work was supported by a Grant-in-Aid for Scientific Research (B)(2), No. 13450255, from the Japan Society for the Promotion of Science. Two of the authors (K. S. and R. Y. U.) would like to thank the Japan Society for Promotion of Science for Young Scientists for support.

[1] G. E. Bacon, I. W. Dunmer, J. H. Smith, and R. Street, Proc. R. Soc. London, Ser. A **241**, 223 (1957).
[2] H. Uchishiba, J. Phys. Soc. Jpn. **31**, 436 (1971).
[3] N. Honda, Y. Tanji, and Y. Nakagawa, J. Phys. Soc. Jpn. **41**, 1931 (1976).
[4] T. J. Hicks, A. R. Pepper, and J. H. Smith, J. Phys. C **1**, 1683 (1968).
[5] T. Yamaoka, J. Phys. Soc. Jpn. **36**, 445 (1974).
[6] R. Yamauchi, T. Hori, M. Miyakawa, and K. Fukamichi, J. Alloys Compd. **309**, 16 (2000).
[7] Y. Endoh and Y. Ishikawa, J. Phys. Soc. Jpn. **30**, 1614 (1971).
[8] T. Yamaoka, M. Mekata, and H. Takaki, J. Phys. Soc. Jpn. **31**, 301 (1971).
[9] R. Yamauchi, K. Fukamichi, H. Yamauchi, and A. Sakuma, J. Alloys Compd. **279**, 93 (1998).
[10] R. Yamauchi, K. Fukamichi, H. Yamauchi, A. Sakuma, and J. Echigoya, J. Appl. Phys. **85**, 4741 (1999).
[11] K. Sasao, R. Yamauchi, K. Fukamichi, and H. Yamauchi, IEEE Trans. Magn. **35**, 3910 (1999).
[12] T. Hori, Y. Tsuchiya, Y. Ishii, and K. Hojyou, J. Phys. Soc. Jpn. **70**, Suppl. A, 142 (2001).
[13] T. Hori, Y. Tsuchiya, S. Funahashi, Y. Shimojyo, H. Shiraishi, K. Hojyou, and Y. Nakagawa, J. Magn. Magn. Mater. **196–197**, 663 (1999).
[14] E. Krén, G. Kádár, L. Pál, J. Sólyom, P. Szabó, and T. Tarnóczi, Phys. Rev. **171**, 574 (1968).
[15] K. Hoshino, R. Nakatani, H. Hoshiya, Y. Sugita, and S. Tsunashima, Jpn. J. Appl. Phys., Part 1 **35**, 607 (1996).
[16] H. N. Fuke, K. Saito, Y. Kamiguchi, H. Iwasaki, and M. Sahashi, J. Appl. Phys. **81**, 4004 (1997).
[17] A. J. Devashayam, P. J. Sides, and M. H. Kryder, J. Appl. Phys. **83**, 7216 (1998).
[18] D. Wang, M. Tondra, C. Nordman, and J. M. Daughton, IEEE Trans. Magn. **35**, 2886 (1999).
[19] S. Tehrani, J. M. Slaughter, E. Chen, M. Durlam, J. Shi, and M. DeHerrera, IEEE Trans. Magn. **35**, 2814 (1999).
[20] A. P. Malozemoff, Phys. Rev. B **35**, 3679 (1987).
[21] N. C. Koon, Phys. Rev. Lett. **78**, 4865 (1997).
[22] T. C. Schulthess and W. H. Butler, J. Appl. Phys. **85**, 5510 (1999).
[23] I. Tomeno, H. N. Fuke, H. Iwasaki, M. Sahashi and Y. Tsunoda, J. Appl. Phys. **86**, 3853 (1999).
[24] J. Kübler, K.-H. Höck, J. Sticht, and A. R. Williams, J. Phys. F: Met. Phys. **18**, 469 (1988).
[25] J. S. Kouvel and J. S. Kasper, in *Proceedings of the International Conference on Magnetism, Nottingham, England, 1964* (The Physical Society, London, 1964), p. 169.
[26] A. Sakuma, J. Phys. Soc. Jpn. **69**, 3072 (2000).
[27] A. Sakuma, J. Phys. Soc. Jpn. **67**, 2815 (1998).
[28] A. I. Liechtenstein, M. I. Katsnelson, V. P. Antropov, and V. A. Gubanov, J. Magn. Magn. Mater. **67**, 65 (1987).
[29] O. K. Andersen and O. Jepsen, Phys. Rev. Lett. **53**, 2571 (1984).
[30] J. Kudrnovský and V. Drchal, Phys. Rev. B **41**, 7515 (1990).
[31] J. Kudrnovský, V. Drchal, and J. Masek, Phys. Rev. B **43**, 4613 (1991).
[32] A. Sakuma, IEEE Trans. Magn. **35**, 3349 (1999).
[33] A. Sakuma, R. Y. Umetsu, and K. Fukamichi, Phys. Rev. B **66**, 014432 (2002).
[34] N. A. Cade and W. Young, J. Phys. F: Met. Phys. **10**, 2035 (1980).
[35] T. Jo and K. Hirai, J. Phys. Soc. Jpn. **55**, 2017 (1986).
[36] R. S. Fishman and S. H. Liu, Phys. Rev. B **59**, 8672 (1999).
[37] T. Yamaoka, M. Mekata, and H. Takaki, J. Phys. Soc. Jpn. **36**, 438 (1974).
[38] R. S. Fishman, W.-T. Lee, S. H. Liu, D. Mandrus, J. L. Robertson, K. J. Song, and J. R. Thompson, Phys. Rev. B **61**, 12 159 (2000).